Infinite Science Publishing

Proceedings Article

Uncertainty estimation for 2D magnetic particle imaging

Mark-Alexander Henn ⓘ[a,b,*] · Klaus Natorf Quelhas[a,c,d] · Solomon I. Woods ⓘ[a]

[a]National Institute of Standards and Technology (NIST), Gaithersburg, MD 20899, USA
[b]University of Maryland, College Park, MD 20742, USA
[c]Instituto Nacional de Metrologia, Qualidade e Tecnologia, Rio de Janeiro, Brazil
[d]Universidade Federal do Rio de Janeiro, Rio de Janeiro, Brazil
*Corresponding author, email: mark.henn@nist.gov

Abstract

Magnetic Particle Imaging (MPI) has in recent years been established as a powerful imaging tool that measures the non-linear magnetic response of magnetic particles to an applied field. Obtaining quantitative information from these images in the form of a discretized version of the particle distribution in space requires the solution of an inverse problem that can be addressed by linear regression. We demonstrate how the linear regression can also be used to estimate the uncertainty of the reconstructed particle distribution.

I. Introduction

The quantitative analysis of data obtained through Magnetic Particle Imaging (MPI)[1–3] usually requires the solution of an inverse problem; the directly measured voltage signal in time is first translated into image data before it is further analyzed to yield the number of particles at a given position in space as a discretized representation of the particle distribution.

This second step in quantitative analysis of the particle concentration distribution requires deconvoluting the image data in order to remove the blur introduced by the Point Spread Function (PSF) of the imaging system, which at its core can be expressed as a linear regression problem as shown in [4]. However, this approach only yields a point estimate of the number of particles at a given spatial position without saying anything about its uncertainties.

In this work, we demonstrate how the linear regression formulation of the inverse imaging problem can easily be used to report uncertainties in a compliant way with the Guide to the Expression of Uncertainty in Measurement [5] adding to a recently submitted paper [6] in which we presented an approach to the uncertainty quantification based on the bootstrap method [7].

II. Methods

We recapitulate the basic methods for simulation and reconstruction, which are similar to those developed in [4].

II.I. Forward Model

If we denote by $\rho(\mathbf{x})$ the particle distribution, by R_0 the nominal sensitivity of the receiver coils, by $\mathbf{G}$ the gradient of the applied gradient field, by $m = \frac{1}{6}\pi M_s d^3$ the magnetic moment of a single particle, by T the temperature in Kelvin, by k_B and μ_0 the Boltzmann constant and the vacuum permeability respectively, and by $\mathbf{r} = \mathbf{r}(t)$ the trajectory of the field free point (FFP), we can calculate

the resulting MPI signal with the equation

$$\mathbf{s}(t) = \mu_0 m R_0 \frac{d}{dt} \int_{\mathbb{R}^3} \rho(\mathbf{x}) \mathscr{L}\left[k \|\mathbf{G}(\mathbf{r}-\mathbf{x})\|\right] \frac{\mathbf{G}(\mathbf{r}-\mathbf{x})}{\|\mathbf{G}(\mathbf{r}-\mathbf{x})\|} d\mathbf{x},$$
(1)

where $\mathscr{L}[\cdot]$ is the Langevin function and $k = \frac{\mu_0 m}{k_B T}$.

II.II. Reconstruction

The reconstruction makes use of the fact that we can spatially fit the time signal data $\mathbf{s}(t)$ to obtain the so-called trace data $\mathbf{u}(\mathbf{x})$, and, once we populate a convolution matrix $\mathbf{K}$ based on the system's PSF, can determine the particle distribution by minimizing the regularized [8] function

$$\chi^2(\boldsymbol{\rho}) = \|\mathbf{K}\boldsymbol{\rho} - \mathbf{u}\|^2 + \lambda\|\boldsymbol{\rho}\|^2.$$
(2)

II.III. Uncertainty Quantification

If we have information on the measurement error on $\mathbf{u}$, such as an estimate for the covariance matrix $\boldsymbol{\Sigma_u}$, that we will call $\mathbf{V}$, we can replace Eq. 2 with a weighted version

$$\begin{aligned}\chi^2_{\mathbf{V}}(\boldsymbol{\rho}) &= \|\mathbf{K}\boldsymbol{\rho} - \mathbf{u}\|^2_{\mathbf{V}} + \lambda_{\mathbf{V}}\|\boldsymbol{\rho}\|^2 \\ &= (\mathbf{K}\boldsymbol{\rho} - \mathbf{u})^{\mathsf{T}}\mathbf{V}^{-1}(\mathbf{K}\boldsymbol{\rho} - \mathbf{u}) + \lambda_{\mathbf{V}}\|\boldsymbol{\rho}\|^2,\end{aligned}$$
(3)

with $\lambda_{\mathbf{V}} = \lambda \cdot \|\mathbf{V}^{-1}\|_F$, and $\|\cdot\|_F$ denoting the Frobenius norm of a matrix. Once we determine the optimal concentration profile $\hat{\boldsymbol{\rho}}$, i.e., the profile that minimizes the $\chi^2_{\mathbf{V}}$ function in Eq. 3, we can give an estimate of the profile's uncertainties by calculating the covariance matrix

$$\boldsymbol{\Sigma}_{\hat{\boldsymbol{\rho}}} = \left(\mathbf{K}^{\mathsf{T}}\mathbf{V}^{-1}\mathbf{K} + \lambda_{\mathbf{V}}\mathbf{E}\right)^{-1},$$
(4)

where $\mathbf{E}$ is the identity matrix of size $n = \dim(\mathbf{u})$. Since the matrix $\mathbf{V}$ is close to singular, we apply a truncated singular value decomposition to calculate its inverse [9].

The uncertainty on an individual point $\hat{\rho}_i$ is then given by the square root of the diagonal elements of $\boldsymbol{\Sigma}_{\hat{\boldsymbol{\rho}}}$.

III. Simulation Setup

We use the forward model from Section II.I with experimental parameters given in Table 1 and the particle distribution shown in Figures 1 a) and b) to generate the input data. The FFPs Lissajous trajectory $\mathbf{r}(t)$ is generated by the drive field

$$\mathbf{H}_D(t) = \left[\mu_0 B_x \sin(2\pi f_x t), \mu_0 B_y \sin(2\pi f_y t), 0\right]^{\mathsf{T}}.$$
(5)

We add white noise with zero mean and a standard deviation of one percent of the maximum value of the signal vector $\mathbf{s}$. We divide the resulting field-of-view into 51×51 pixels, which leads to the following sizes of the vectors $\mathbf{u}, \boldsymbol{\rho} \in \mathbb{R}^{2601}$, and matrices $\mathbf{K}, \mathbf{V} \in \mathbb{R}^{2601 \times 2601}$, involved.

Table 1: Simulation Parameters.

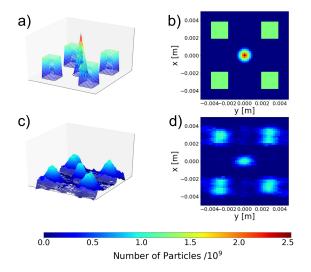| Particle Diameter	d	$2 \cdot 10^{-8}$ m
Saturation Magnetization	M_s	$4.5 \cdot 10^5$ A/m
Temperature	T	293 K
Gradient Field Amplitudes	G_x	8 T/m
	G_y	-4 T/m
Drive Field Amplitudes	B_x	$4 \cdot 10^{-2}$ T
	B_y	$2 \cdot 10^{-2}$ T
Excitation Field Frequencies	f_x	25.5 kHz
	f_y	25.25 kHz
Coil Sensitivity	R_0	$8.38 \cdot 10^{-4}$ T/A
Regularization Parameter	λ	10^8

Figure 1: a) Phantom used in simulations, b) top-down view of phantom, c) reconstructed particle distribution $\hat{\boldsymbol{\rho}}$ d) top-down view of reconstructed particle distribution, note the different resolution in x and y directions, particularly for the small central cone, due to different gradient fields.

IV. Results

We now apply the reconstruction and uncertainty estimation algorithms to the noisy simulation data introduced in the previous Section.

IV.I. Error Analysis

As we have seen in Section II.III, to determine the uncertainty in the reconstructed particle distribution we need an estimate of the measurement uncertainty for the trace data $\mathbf{u}$, which is a function of the time signal data (see Figure 2 for the comparison between $\mathbf{s}(t)$ and $\mathbf{u}$). Since there is no direct way to determine how the noise propagates, we perform a Monte Carlo (MC) [10] analysis, i.e., we generate multiple noisy realizations of the

time signal data, calculate the corresponding trace data and determine the sample variance from these. Since the spatial fitting is less time-consuming than solving the regression problem, there is a notable time advantage compared to the bootstrap method. Note, that in the case of real measured data we can compute the trace data from multiple noisy measurements and then determine the sample variance.

The results in the form of the reconstructed particle distributions, along with the calculated 95% confidence intervals are shown in Figure 3. As expected, the error bars cover the ground truth, showing the reconstruction's reliability and the estimated parameter uncertainties.
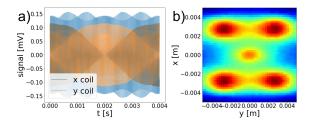

Figure 2: a) Raw signal data **s**, b) trace data **u** after spatial fitting
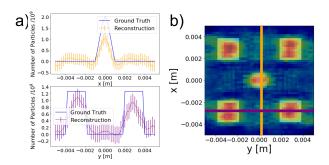

Figure 3: a) Reconstruction with expanded 95% confidence intervals, as required we see good coverage of the ground truth. b) Location of line scans for the reconstruction in a) are shown overlaid on the top-down view of the reconstruction that is itself overlaid with a transparent top-down view of the ground truth schematic

V. Discussion and Conclusion

In this presentation, we have shown how to improve the quantitative analysis of MPI data by calculating the associated uncertainties of the reconstructed particle distribution. This improvement can be achieved by using the linear regression formulation of the underlying inverse problem, which establishes a relation between the uncertainties in the measurement and the uncertainties in the reconstructed parameters.

However, in the case of MPI, the raw input data (the time signal data) is first fitted to a spatial grid before being used for the reconstruction. In order to estimate the magnitude of the error on the spatially fitted data, we performed a MC simulation and used the sample variance as weights for our estimation. With these adjustments, we were able to recover the ground truth distribution within the error bars of the reconstruction. Future work might circumvent the MC simulation by using a maximum likelihood estimation [11] that determines the noise from the spatially fit data itself.

Acknowledgments

Author's statement

Conflict of interest: Authors state no conflict of interest.

References

[1] B. Gleich and J. Weizenecker. Tomographic imaging using the nonlinear response of magnetic particles. *Nature*, 435(7046):1214–1217, 2005, doi:10.1038/nature03808.

[2] T. Knopp and T. M. Buzug, Magnetic Particle Imaging: An Introduction to Imaging Principles and Scanner Instrumentation. Berlin/Heidelberg: Springer, 2012, doi:10.1007/978-3-642-04199-0.

[3] T. Knopp, N. Gdaniec, and M. Möddel. Magnetic Particle Imaging: from Proof of Principle to Preclinical Applications. *Physics in Medicine & Biology*, 62:R124–R178, 2017, doi:https://doi.org/10.1088/1361-6560/aa6c99.

[4] T. März and A. Weinmann. Model-based reconstruction for magnetic particle imaging in 2d and 3d. *Inverse Problems & Imaging*, 10(4):1087, 2016.

[5] W. Bich, M. G. Cox, R. Dybkaer, C. Elster, W. T. Estler, B. Hibbert, H. Imai, W. Kool, C. Michotte, L. Nielsen, *et al.* Revision of the 'guide to the expression of uncertainty in measurement'. *Metrologia*, 49(6):702, 2012.

[6] M.-A. Henn, K. Quelhas Natorf, T. Q. Bui, and S. I. Woods. Improving Model-Based MPI Image Reconstructions: Baseline Recovery, Receive Coil Sensitivity, Relaxation and Uncertainty Estimation. *International Journal on Magnetic Particle Imaging*, submitted for publication.

[7] B. Efron and R. J. Tibshirani, An Introduction to the Bootstrap. CRC Press, 1994,

[8] A. N. Tikhonov, On the Solution of Ill-Posed Problems and the Method of Regularization, in *Doklady Akademii Nauk*, Russian Academy of Sciences, 151, 501–504, 1963.

[9] P. C. Hansen. The truncatedsvd as a method for regularization. *BIT Numerical Mathematics*, 27(4):534–553, 1987.

[10] W. Bauer. The Monte Carlo Method. *Journal of the Society for Industrial and Applied Mathematics*, 6(4):438–451, 1958.

[11] J. J. O. Ruanaidh and W. J. Fitzgerald, Numerical Bayesian methods applied to signal processing. Springer Science & Business Media, 2012,